Electronic supplementary information

A new molecular material as dopant-free hole transporting layer for stable perovskite solar cells

Rui Zhang [a, 1], Jiang-Yang Shao [b, 1], Bingcheng Yu [a], Hongshi Li [a], Yu-Wu Zhong [b] *, Jiangjian Shi, [a, d, e] Yanhong Luo, [a, d, e] Huijue Wu, [a] Dongmei Li [a, d, e]*, Qingbo Meng [a, c, d, e]*

[a] *Key Laboratory for Renewable Energy (CAS), Beijing Key Laboratory for New Energy Materials and Devices, Beijing National Laboratory for Condense Matter Physics, Institute of Physics, Chinese Academy of Sciences, Beijing, 100190, China*

[b] *Beijing National Laboratory for Molecular Sciences, CAS Key Laboratory of Photochemistry, CAS Research/Education Center for Excellence in Molecular Sciences, Institute of Chemistry, Chinese Academy of Sciences, Beijing, 100190, China*

[c] *Center of Materials Science and Optoelectronics Engineering, University of Chinese Academy of Sciences, Beijing 100049, China*

[d] *School of Physics Science, University of Chinese Academy of Sciences, Beijing 100049, China*

[e] *Songshan Lake Materials Laboratory, Dongguan 523808, China*

E-mail addresses: zhongyuwu@iccas.ac.cn (Y.-W. Zhong), dmli@iphy.ac.cn (D. Li), qbmeng@iphy.ac.cn (Q. Meng)

[1] These authors contribute equally to this work.

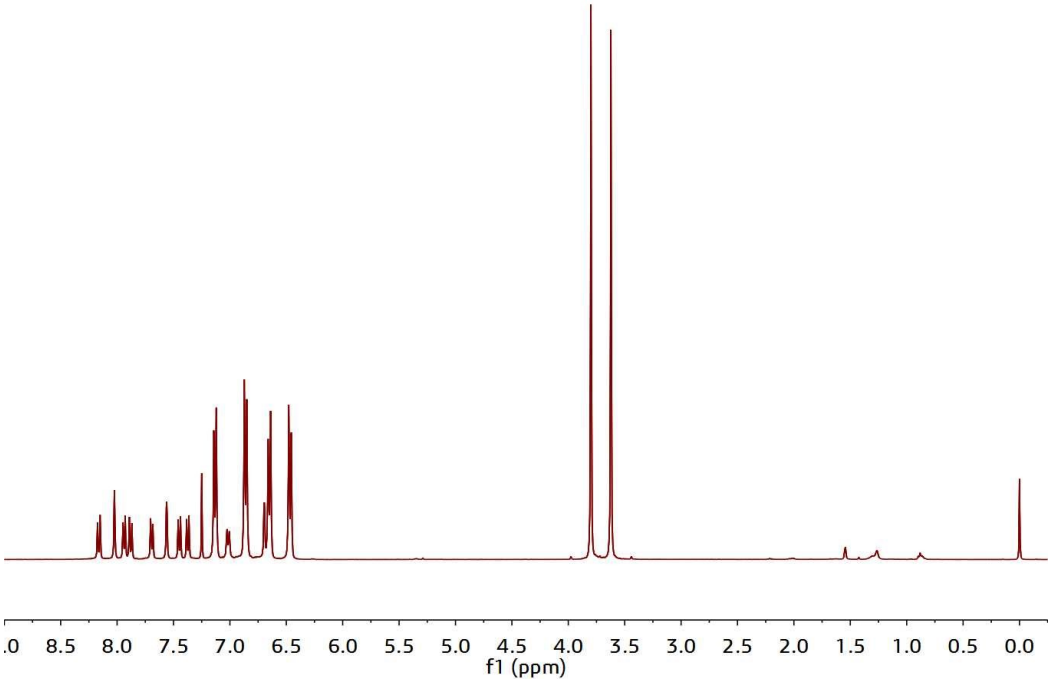

Fig. S1. ^{1}H NMR of PFD

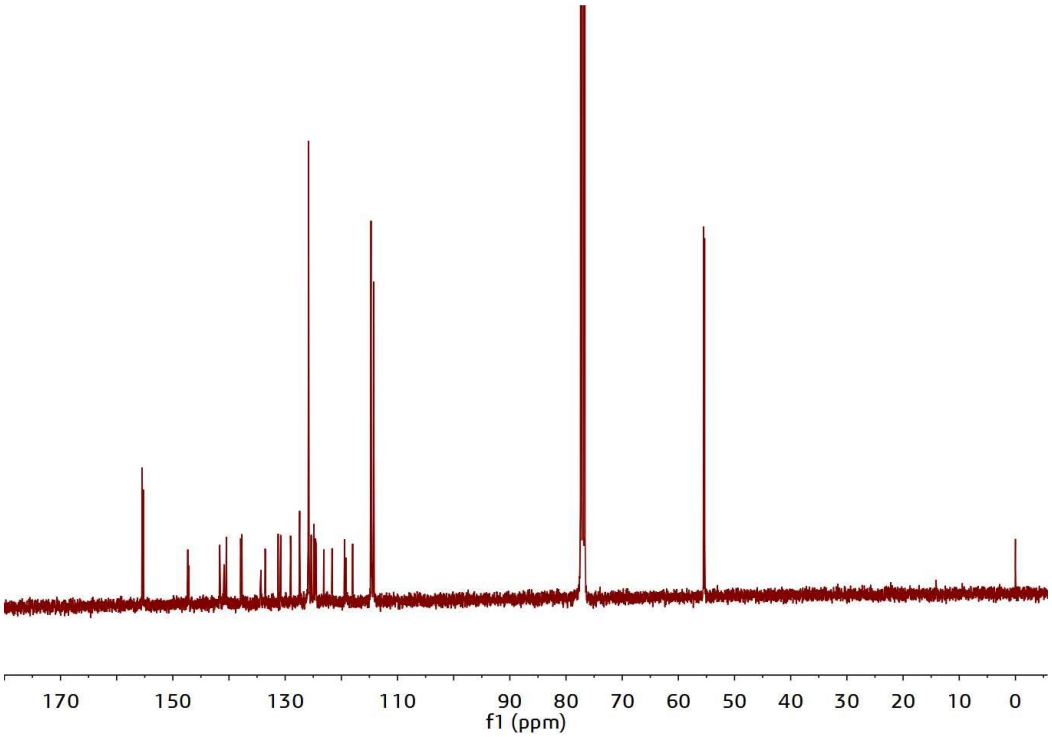

Fig. S2. ^{13}C NMR of PFD

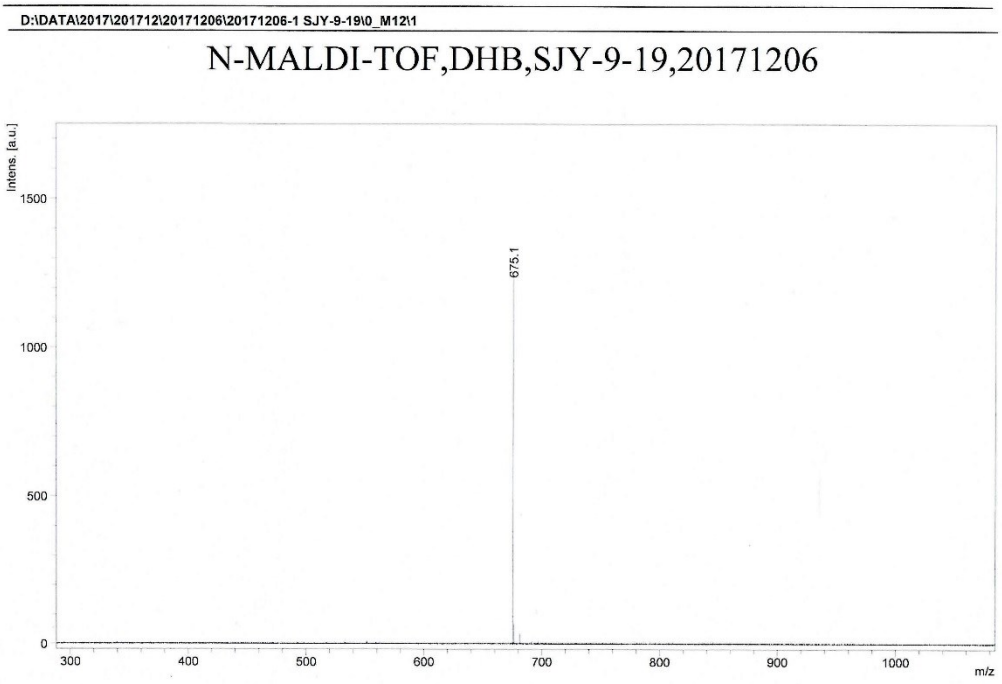

Fig. S3. Mass spectrum of compound 2

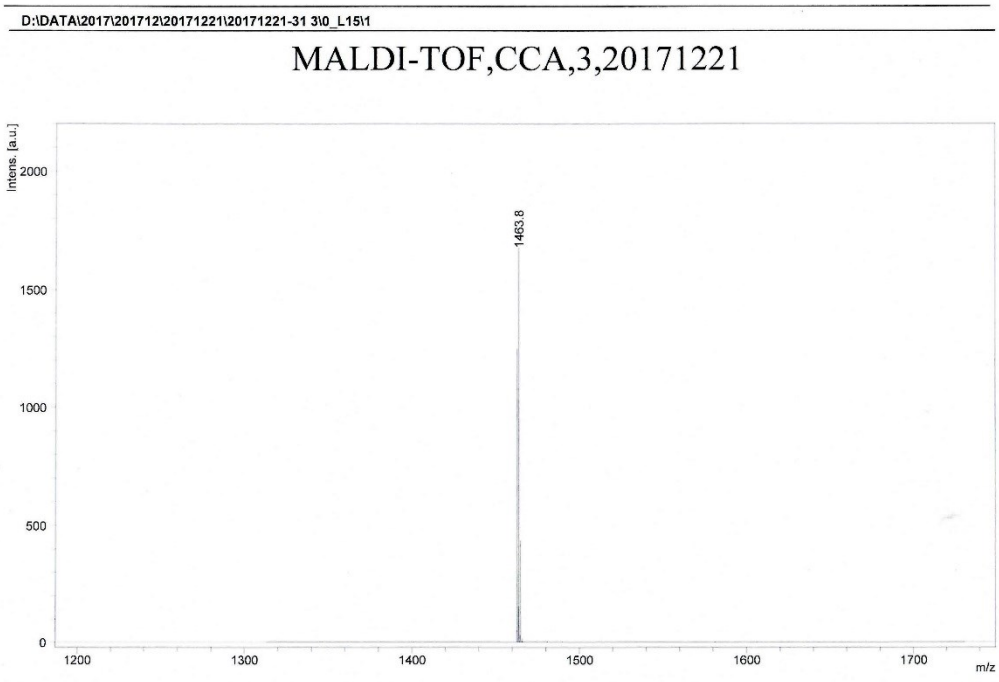

Fig. S4. Mass spectrum of PFD

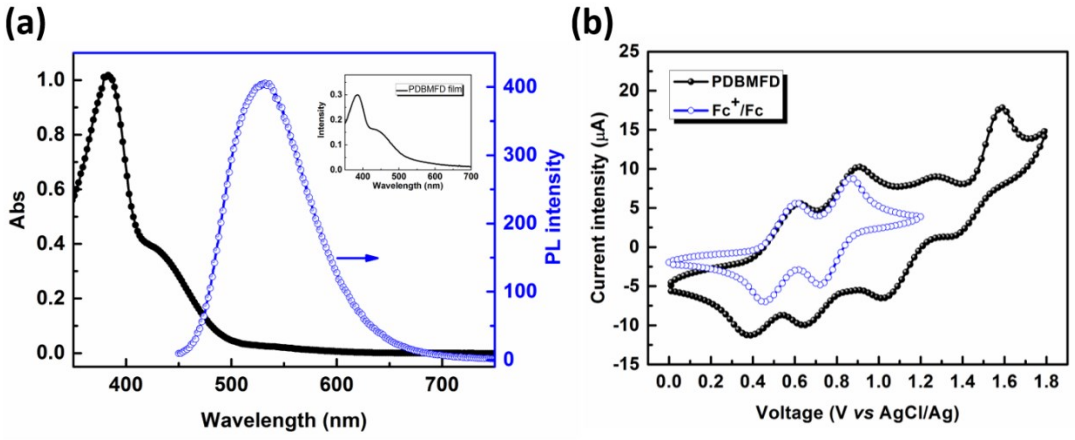

Fig. S5. (a) UV-visible spectrum and steady-state photoluminescence (PL) spectrum of PDBMFD in dichloromethane (solution concentration: 1×10^{-5} M); (b) Cyclic voltammograms of PDBMFD in dichloromethane in which Pt wire as working electrode, Pt wire as counter electrode and AgCl/Ag as reference electrode, and the system was calibrated by a ferrocenium/ferrocene ($FeCp_2^{0/+}$) as redox couple.

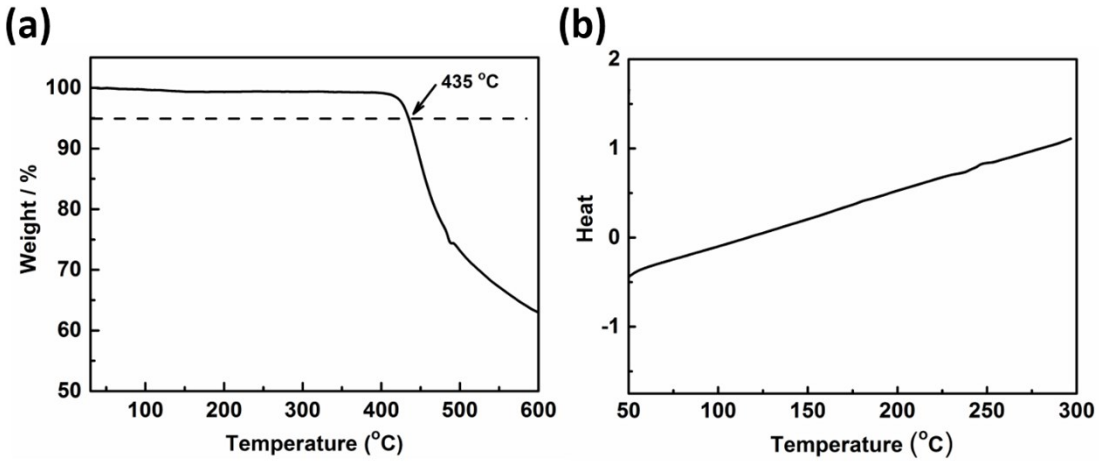

Fig. S6. (a) TGA and (b) DSC curves of the PFD

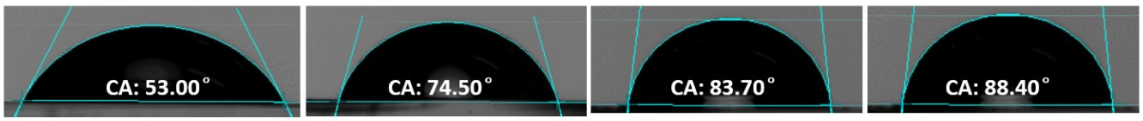

Fig. S7. Contact angles of four films, (a) perovskite, (b) perovskite/PFD, (c) perovskite/spiro-OMeTAD, (d) perovskite/PFD/spiro-OMeTAD films, using glycerol as solvent.

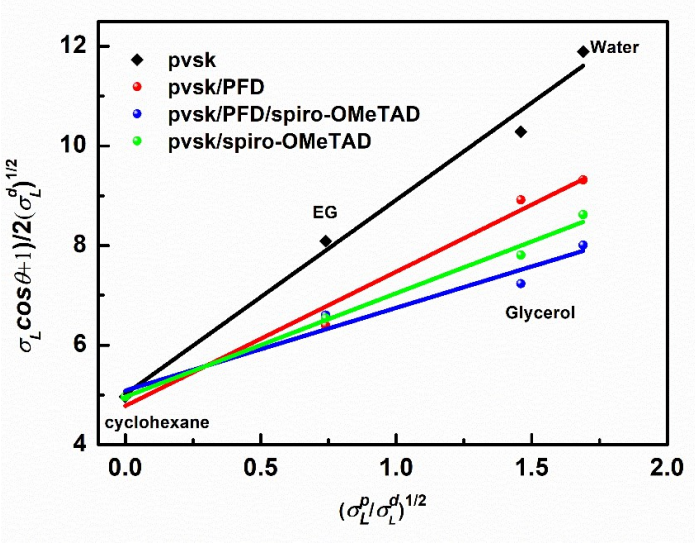

Fig. S8. The OWRK plots for the surface energy of these four films, each point reflects the interaction between the film surface and the specified liquids (EG: ethylene glycol). The solid line are linear fittings.

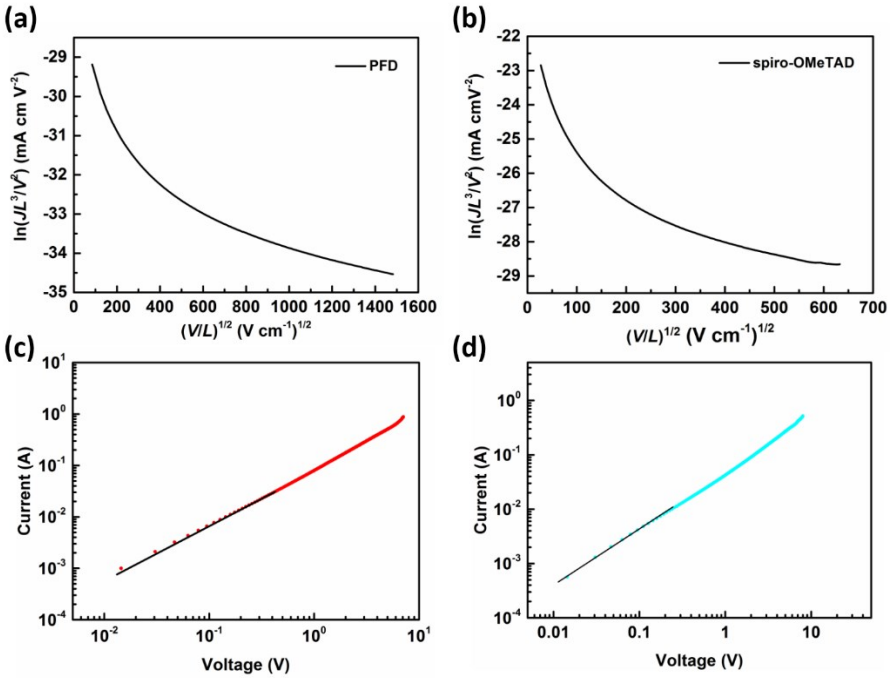

Fig. S9. Dark *J-V* characteristics of hole-only devices based on dopant-free PFD (a) and (c) or *spiro*-OMeTAD (b) and (d).

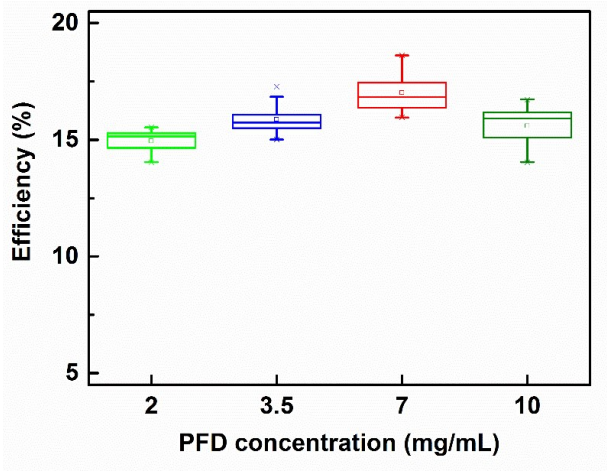

Fig. S10. The box statistics diagram of the 20 cells based on different PFD concentrations.

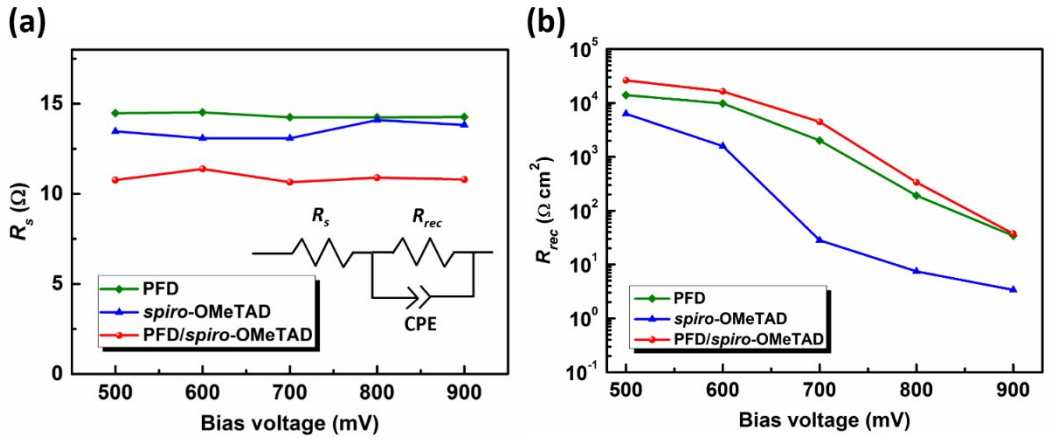

Fig. S11. (a) R_s versus bias voltage of the three devices; (b) Plots of the recombination resistance (R_{rec}) *vs*. bias voltage for the devices with PFD, *spiro*-OMeTAD and PFD/*spiro*-OMeTAD. Inset: Equivalent circuit for fitting EIS spectra.

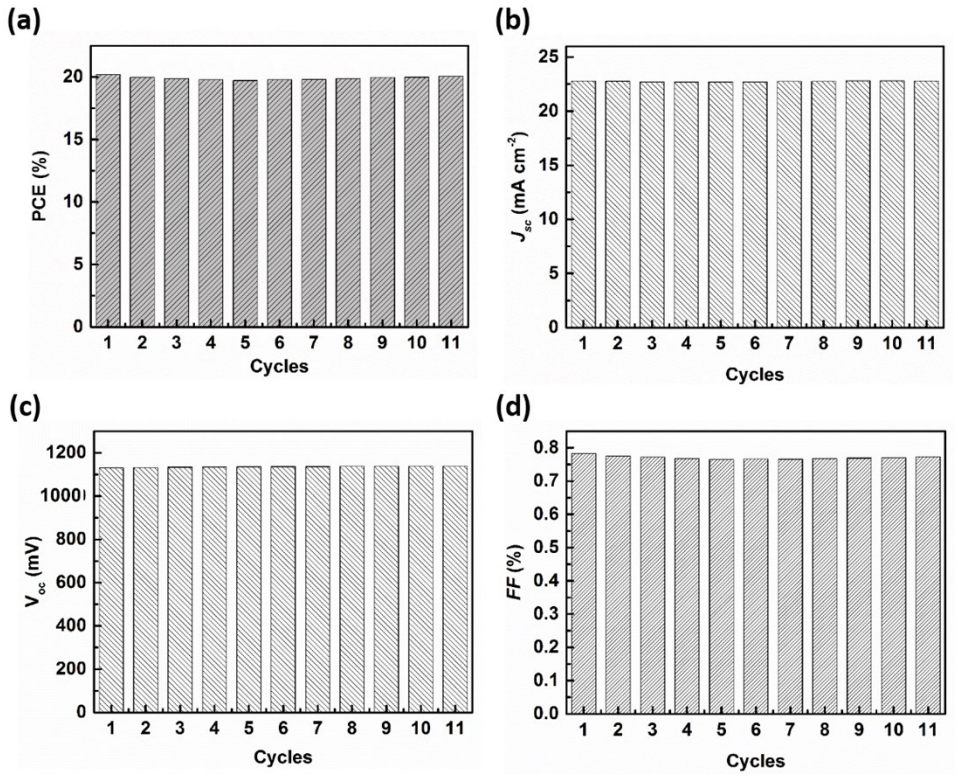

Fig. S12. Photovoltaic parameters (PCE, J_{sc}, V_{oc} and *FF*) *versus* multiple scanning cycles under continuous *J-V* scanning under AM 1.5 illumination (100 mW cm^{-2})

Table S1. Photovoltaic parameters of the champion devices based on different PFD concentrations

PFD concentration (mg/mL)	J_{sc} (mA cm^{-2})	V_{oc} (mV)	*FF*	Eff (%)
2	22.08	997	0.705	15.53
3.5	22.82	1074	0.705	17.29
7	22.81	1086	0.751	18.60
10	23.27	1070	0.672	16.73